Verification of the dispersive charge transport in a hydrazone:polycarbonate molecularly doped polymer

2009 J. Phys.: Condens. Matter 21 115107

(http://iopscience.iop.org/0953-8984/21/11/115107)

IOP PUBLISHING JOURNAL OF PHYSICS: CONDENSED MATTER

J. Phys.: Condens. Matter **21** (2009) 115107 (7pp) doi:10.1088/0953-8984/21/11/115107

Verification of the dispersive charge transport in a hydrazone:polycarbonate molecularly doped polymer

Andrey P Tyutnev[1], Vladimir S Saenko[1], Evgenii D Pozhidaev[1] and Vladislav A Kolesnikov[2,3]

[1] Moscow State Institute of Electronics and Mathematics, Bol. Trechsvyatitel. per., 3, Moscow 109028, Russia

[2] Frumkin Institute of Physical Chemistry and Electrochemistry, Russian Academy of Sciences, Leninskii Prospekt, 31, Moscow 119991, Russia

Received 21 July 2008, in final form 12 December 2008
Published 9 February 2009
Online at stacks.iop.org/JPhysCM/21/115107

Abstract

We report results of specially planned experiments intended to verify the dispersive character of the charge carrier transport in polycarbonate molecularly doped with hydrazone at 30 wt% loading, using for this purpose samples specifically featuring a well-defined plateau on a linear–linear plot. For this purpose we propose a new variant of the time-of-flight technique which allows easy changing of the generation zone width from about 0.5 μm (surface excitation) through intermediate values to full sample thickness (bulk excitation). To achieve this, we use electron pulses of 3–50 keV energy rather than traditional light pulses provided by lasers. Experimental results corroborated by numerical calculations uniquely prove that carrier transport in this molecularly doped polymer is dispersive, with the dispersion parameter equal to 0.75. Nevertheless, the mobility field dependence follows the famous Poole–Frenkel law.

1. Introduction

Charge carrier transport in molecularly doped polymers (MDP) has been extensively studied since the 1970s but still seems to be not properly understood. It suffices to say that at least 5–7 theories are in use for interpretation of the field, temperature and concentration (of dopant molecules) dependences of the drift mobility of charge carriers [1–6]. Of course, two main competing theories need to be noted. These are Gaussian disorder model (GDM) [3, 4] and multiple trapping model with an exponential distribution (MT) [2] or an equivalent Scher–Montroll (SM) [1] hopping formulation. Recently, GDM has been criticized [7].

The major existing controversy concerns the interpretation of a flat plateau (sometimes a sloping shoulder or a cusp, which is a current rising gradually after an initial spike to a peak before decaying into the tail) frequently appearing on the time-of-flight (TOF) curves plotted on a linear current–linear timescale, allowing straightforward determination of the transit time. GDM treats this fact as indicating the attainment of the quasi-equilibrium condition [5]. On the other hand, there is a point of view that regards the plateau as an artifact due to delayed emission from surface traps [8–10].

Supporters of the GDM dismissed the early results, which established the very concept of the dispersive transport in MDP, on the ground that the samples used did not meet the purity requirements. Researchers began to qualify for research only those samples, which featured a well-defined kink on the TOF transient, be it a flat plateau (ideal case), slightly sloping or even gently cusping shoulders marking the time of flight on a linear scale. Such an approach has been universally accepted and GDM formalism became an instrument to interpret and parameterize TOF experiments on MDP.

Our recent work with hydrazone-doped polycarbonate revealed that the real situation with MDP transport may not be that definitive [11, 12]. First, we introduced in the field an electron gun source to replace the traditional lasers. This step allowed us to realize surface (TOF) as well as the bulk (TOF-2) generation of carriers (the last feature is practically unattainable with lasers). Second, we stressed the importance of presenting TOF data on double logarithmic plots. Both innovations proved decisive in establishing the true nature of carrier transport in this particular MDP as being dispersive.

[3] Deceased.

Unfortunately, TOF traces in more than 50 samples were mainly amenable to analysis by means of double logarithmic scale and only two had flat plateaus. But, what is important is the fact that drift mobilities in our samples and plateau-containing ones described in the literature [5] were very close, suggesting that their quality was substantially the same.

To remove this last barrier concerning MDP sample quality we decided to use coating strips made at Eastman Kodak to prepare test samples, which, judging from already published results [5], should have a very high probability of producing TOF transients with flat plateaus on a regular basis.

In this paper we decided to repeat these electron-gun-based experiments on the above samples using not only TOF and TOF-2 techniques as in [11, 12] but also a newly developed variation of these two, the so-called TOF-1a method employing a sequence of measurements with generation zone length gradually increasing from almost zero to the full sample length. This paper reports the results of these experiments, gives a general overview of the theory and concludes with a discussion.

2. Experimental details

As stated earlier, layers of polycarbonate (PC) molecularly doped with 30 wt% of diethylaminobenzaldehyde–diphenylhydrazone (DEH) were coated at Eastman Kodak on 180 μm thick polyethyleneterephthalate films equipped with a thin semitransparent Ni layer as described elsewhere [13, 14]. MDP layers were 10–19 μm (mostly 14–16 μm). The sheets have been cut to order in Moscow. The sample's diameter was 40 mm while the upper Al electrodes of 26 mm in diameter were thermally evaporated in vacuum to 50–100 nm in thickness.

Experiments were conducted using the electron gun source ELA-65 [11, 12]. This facility was operated in a single-pulse regime. Electron energy could be easily adjusted from 3 to 50 keV so that both TOF (surface generation) and TOF-2 (bulk generation) techniques were readily realized simply by changing electron energy (electron range at 50 keV is sufficiently large to ensure almost uniform irradiation of polymer films no thicker than 25 μm). However, unlike our previous studies, the main emphasis in this work has been placed on a new variant of the TOF technique consisting in a step-wise increase of electron energy, allowing one to gradually increase the width of the generation zone from 0.5 μm to the full sample length. As we will see later, such an approach allows easy discrimination between two transport modes.

Pulse length was 25 μs and beam current density (up to 1 mA cm^{-2}) was easily made to order. The irradiated spot (20 mm in diameter) contrasts favorably with the laser technique (about 1 mm in diameter) thus considerably mitigating space charge effects. The electron pulse starts 14 μs after the trigger signal clearly marking the zero line. Standard electron energy for TOF experiments is 7 keV.

The facility requires no special radiation shielding, takes only moderate room space and a researcher can sit by it during an experimental run. Irradiation of polymer samples took place in a vacuum chamber ($\sim 3 \times 10^{-2}$ Pa) of the ELA-65 facility at room temperature only.

We believe that electron guns are ideal instruments for the study of carrier transport. Spear [15], Gross [16] and Hirsch [17] have pioneered using electron guns as universal tools to probe charge carrier transport in conventional non-photoconductive dielectrics.

To obtain data allowing an unequivocal interpretation, one needs to carry out measurements in a small signal regime so that the applied electric field remains unperturbed and no carrier loss to bimolecular recombination occurs. In our experiments parameter q, giving the ratio of the surface density of the generated free carriers to that of the charge residing on electrodes, was normally less than 0.1.

The current mode should be preferred. So, the RC time constant should be kept as small as possible. In general, a delicate compromise between numerous experimental factors (load resistor, beam current density, pulse length, irradiated area of the sample, applied electric field, etc) should be sought. Again, using fast electrons as an ionizing agent appreciably facilitates this task.

To improve data collection and processing capability of the measuring circuit we used a computer-assisted electronic scheme, which reads data points at a rate of 4×10^5 s^{-1} up to 10 s and stores them as a computer file to be electronically processed. A printout is ready within minutes after an experimental run. It is important that this scheme is completely safe against electrical breakdown of the sample.

3. Experimental results

3.1. The shape of TOF and TOF-2 current transients

As expected, all samples tested (five in all) produced TOF curves with notable plateaus of all three forms mentioned earlier, a cusp being the most frequent feature. However, the most valuable were two samples with flat plateaus.

Figure 1 presents a TOF curve featuring such a plateau. We used the standard procedure for determination of the relative tail width $W = \frac{t_{1/2}-t_0}{t_{1/2}}$ (two characteristic times t_0 and $t_{1/2}$ are given on the figure). The mobility value, defined by the former time (traditionally cited in the literature), is 0.85×10^{-10} m^2 V^{-1} s^{-1} and compares favorably with the value 1.0×10^{-10} m^2 V^{-1} s^{-1} reported in [18] for 30% DEH in PC at 43 V μm^{-1} and room temperature. $W = 0.46$ is also a typical value for molecularly doped PC generally [5], and specifically 0.44 in [19], 0.52 in [20] but 0.31 in [18].

Nevertheless, we did not confine ourselves to this traditional data reduction and extended it using a double logarithmic representation (figure 2). Here one may see the current at early times during the pulse and immediately after it. Time constant RC of the measuring circuit was about 5 μs, so that at times exceeding 0.1 ms the current transient reproduces approximately an MDP response to δ-pulse irradiation.

Inspection of this figure shows that current falls after the pulse striving to get flat, thus suggesting an equilibration of the hole transport. But after the transit it reveals features uncharacteristic of the quasi-equilibrium transport.

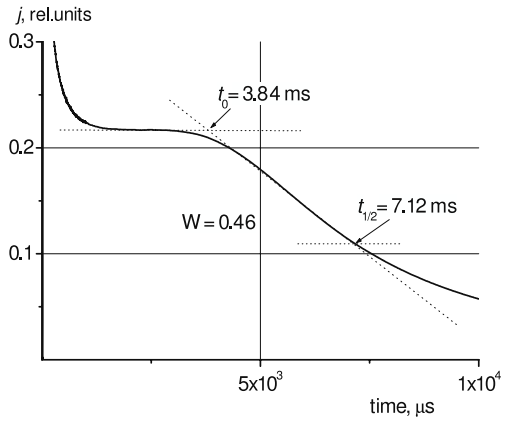

Figure 1. TOF curve for sample no. 1 (thickness 14 μm). Applied voltage 600 V, field 42.8 V μm^{-1}, $RC \approx 5$ μs. This transient matches the best flat plateaus reported in the literature (see, for example, figures 32, 55 and 85 in [5] and [12]). In determining W, it is important that the lower tangent passes as closely as possible through the $t_{1/2}$ data point (usually it takes two or three iterations to achieve this).

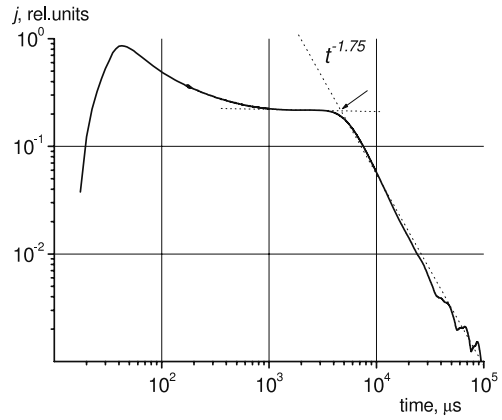

Figure 2. As figure 1 except on double logarithmic scale. Time of flight (5 ms) defined by the intersection of the plateau with the post-flight decay asymptote is indicated by an arrow. Parameter $q = 0.07$ and the free ion yield is 1.6 per 100 eV of absorbed energy. The almost rectangular pulse starts 15 μs after triggering of the computer system and ends 25 μs later, i.e. at $t = 40$ μs.

The current fall follows a power, rather than a near-exponential, time dependence characteristic of the equilibrated transport [4, 21, 22] (see also [12]). The latter feature strongly favors the dispersive transport. Note that this current decay according to a power law proceeds for more than a decade in time, causing the current to diminish by a factor of 200. In addition, the corresponding time of flight indicated by an arrow (5 ms) is effectively bracketed by two TOF values given on figure 1. Thus, we face a dilemma of which type of transport to prefer. Figure 2 shows that the current maximum occurring at $t = 40$ μs coincides with the end of the electron pulse. An important observation is that current decay may well be approximated by a power law $j \propto t^{-1.75}$, the exponent being accurate to ± 0.02.

According to the GDM approach one has to use linear–linear plots, determine drift mobility and, through parameter W, the diffusivity and finally apply GDM formulae to extract model parameters: σ—the energetic width of the hopping site manifold, μ_0—the mobility prefactor, Σ—the positional disorder parameter and C—the famous Poole–Frenkel coefficient entering the ubiquitous $\ln \mu \propto \text{const} + C F_0^{1/2}$ field dependence [4, 5]. The success of such an approach is well known as well as its long-standing (and still unresolved) puzzle concerning the above-mentioned ubiquitous square root field dependence of the drift mobility (see the review [7]). Yet we intend to challenge this approach.

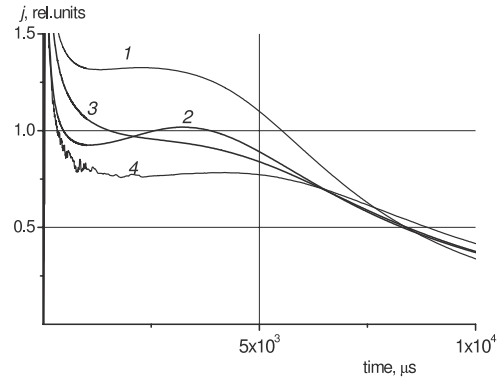

Figure 3. TOF curves for four samples (nos.1–4, Al electrodes) 14, 17.5, 14 and 15 μm thick, respectively, cut from the same coating strip. Applied field 4×10^7 V m^{-1}, load resistor 20 kΩ ($RC \approx 20$ μs), electron beam current density 6.4 μA cm^{-2} and $q = 0.11$ for curve 2. Note that all transients are computer registered ones; simply curves 1–3 happen to be noiseless.

The first indication against GDM has already been mentioned. The next one comes from the occurrence frequency of the various plateau shapes among a group of four samples cut from the same coating strip (figure 3). Here we see that at 40 V μm^{-1} only one has a flat plateau (it was shown in figure 1 at a slightly different field), two have cusps and one has a shoulder.

It is widely recognized that gently sloping plateaus present no difficulty for data processing along traditional lines [18, 20, 23], whereas the frequent appearance of cusps should be regarded as a serious challenge to the theory. It is well known that cusps are not predicted by GDM [4]. Remember that we are always treating the small signal regime. As figure 4 shows, cusps are not influenced by the e-beam intensity and even at its lowest value (curve 3 with $q \approx 0.002$) the cusp for sample no. 2 is still there and looks unchanged. It follows that cusp formation is not due to the famous Many–Rakavy effect (space charge limited currents with $q \gg 1.0$).

Of course, such variability of TOF shapes is a challenge for any theory, not specifically the GDM. Our next task is to find a property that is constant among such samples, of course, within an experimental uncertainty (approximately 20%).

Such a property indeed exists and easily manifests itself once the bulk rather than surface generation mode is used [11, 12]. Optical excitation universally employed to conduct TOF measurements clearly denies an experimentalist such an opportunity. The best tool for this purpose is an electron gun. Changing beam energy from 3 keV

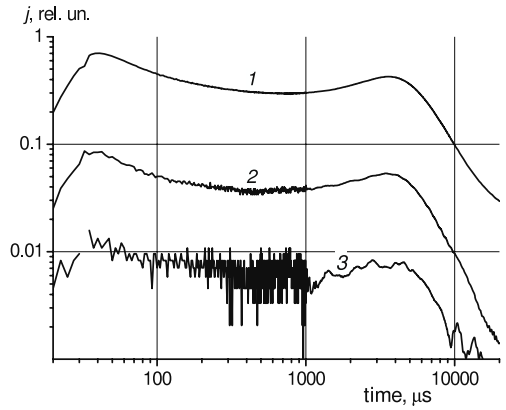

Figure 4. TOF curves for sample no. 2 (thickness 17.5 μm). Applied voltage 700 V, $RC \approx 7.5$ μs. Electron beam current density 3.2 (1), 0.32 (2) and 0.064 μA cm^{-2} so that q declines from approximately 0.1 (1) to 0.01 (2) and 0.002 (3), respectively. This figure graphically illustrates how noise level reduces with rising beam current.

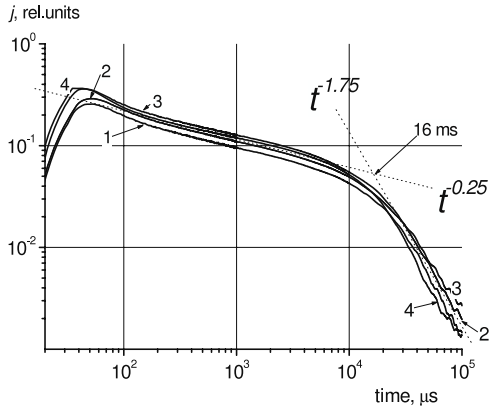

Figure 5. As figure 3 except TOF-2 experiment (electron energy 40 keV). Applied field 4×10^7 V m^{-1}, load resistor 10 kΩ ($RC \approx 10$ μs) on double logarithmic scale.

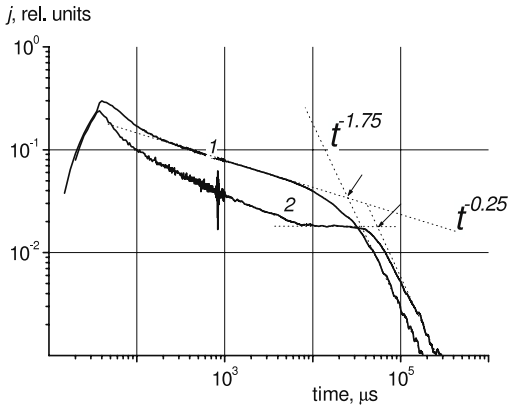

Figure 6. Comparison of TOF-2 (1) and TOF (2) curves for sample no. 1. Applied voltage 200 V, load resistor 10 kΩ ($RC \approx 10$ μs), electron beam current density 3.2 μA cm^{-2} for curve 1. Arrows indicate times of flight: 25 (1) and 54 ms (2), respectively. The curves have been displaced vertically to ease comparison of their shapes.

(surface generation) to 50 keV (near uniform for samples no thicker than 25 μm) provides an easy changeover from TOF to TOF-2. Other major experimental advantages of electron gun sources over laser-based techniques are the absence of any limitations as far as ionization of dopant molecules is concerned (so there is no need to use a special generation layer) and the fact that electrons, unlike photons, have a well-defined maximum range, which is very important. The main disadvantage is, of course, that electron guns are not readily available and are rather expensive to run. The more valuable is information gained in this way.

As found earlier [10–12] and confirmed in the present investigation the property sought is the TOF-2 signature (figure 5). We see that, unlike TOF curves (figure 3), TOF-2 transients are very similar. Yes, there is some scatter among curves, especially after the transit time, but in their central part from 0.2 to 4 ms they all run as power functions $j \propto t^{-0.25}$ slightly differing in magnitude. In a specially constructed experiment (electric field 4 V μm^{-1} and electron current being 10 times larger) we managed to extend this time interval from 0.1 to 100 ms covering three decades.

If interpreted in the framework of MT (or SM) formalism we should assign a value of 0.75 to the dispersion parameter α. Then the current fall should follow a relationship $j \propto t^{-1.75}$, which it really does both in TOF and TOF-2 experiments (figures 2, 5 and 6).

3.2. TOF-1a data

Thus far, we have shown that Kodak samples behave very similar to 30% DEH:PC samples tested earlier as far as TOF-2 and post-transit TOF decays are concerned [11, 12], suggesting that the dispersive rather than Gaussian transport prevails in them as well, irrespective of the plateau appearance. Now we intend to prove this assertion beyond reasonable doubt and, in passing, obtain preliminary information concerning the plausible reasons for plateau formation.

To achieve this we gradually increase the electron energy. As a result, the width of the generation zone is increased as well and it extends more and more into the bulk and away from the metal–polymer interface. In this way we seek to reduce the interface effects in TOF measurements.

Two typical TOF-1a runs are represented in figures 7 and 8. Curves 1–3 on the first figure allow the easy determination of t_0, $t_{1/2}$ and W. For curve 4 this procedure needs some caution while transients 5 and 6 are totally featureless denying such an approach. It is seen that the flat plateau for the first two curves gradually gives way to gently (3) and then strongly (4) sloping plateaus (shoulders) which end up as featureless curves (5, 6).

A similar sequence of events could be seen in figure 8 with the only difference being that the starting shape in this case is a cusp. Note that in between it changes to a flat plateau (somewhere between 3 and 4) and than repeats the changing order observed earlier in figure 7. As we will see later, these results are of paramount importance.

To quantify TOF-1a experiments one needs to relate electron energy to the width of the ensuing generation zone. For electron energies E_e from 3 to 70 keV the following

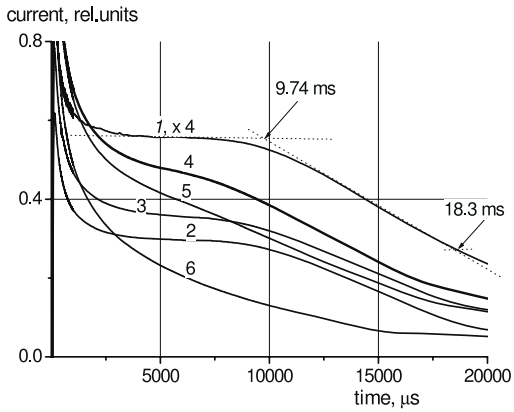

Figure 7. TOF-1a curves for sample no. 5 (8 μm thick). Electron energy 3.4 (1), 7 (2), 9 (3), 11.5 (4), 18.4 (5) and 34.5 keV (6). Electric field 2×10^7 V m^{-1}, load resistor 20 kΩ ($RC \approx 20$ μs), electron beam current density 6.4 μA cm^{-2}. All curves except 1 are given to scale. Inversion in the amplitude sequence for curves 5 (slight) and 6 (strong) is due to the fact that maximum electron range approaches (5) and exceeds (6) the sample length.

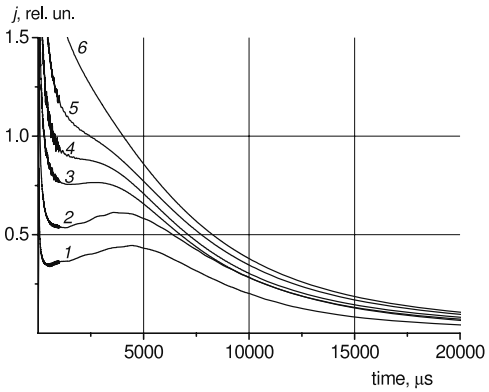

Figure 8. TOF-1a curves for sample no. 2. Electron energy 4.6 (1), 7 (2), 11.5 (3), 13.8 (4), 17.3 (5) and 23 keV (6). The last four curves are given to scale while the first two are multiplied by 1.5. Due to increased sample thickness (17.5 μm) no inversion in amplitude sequence occurs.

relation $l_\mathrm{m} \propto E_\mathrm{e}^{1.67}$ holds, where l_m is the maximum electron range [24]. Specifically in our MDP $l_\mathrm{m} \approx 31$ μm at electron energy $E_\mathrm{e} = 43$ keV [25]. This means that at 7 keV we have the maximum electron range of 1.5 μm, at 12 keV it rises to 3.7 μm and at 20 keV to 8.6 μm.

Within the generation zone, the spatial distribution of pulse generated charge carriers is rather non-uniform. If their concentration at the surface is taken to be unity, it rises to a maximum 2.3 at $\approx 0.35 l_\mathrm{m}$ and then falls off to zero at l_m (it is already very small at $0.8 l_\mathrm{m}$, which is usually taken as a practical range) [25].

We also examined the mobility field dependence at two electron energies (figure 11). In both cases (7 and 23 keV) it was of a Poole–Frenkel type with the parameter $C \approx 4.6 \times 10^{-3}$ (cm V^{-1})$^{1/2}$.

4. Discussion

4.1. Transient shape

Let us look more carefully at the basics of the main TOF technique. It is evident that the mainstream TOF method should be preferred if no controversy is expected. TOF theory is simple and data processing is straightforward. However, in reality this controversy is always there in the form of surface traps and surface layers (interface trapping) [8, 9].

Unlike this, in the case of TOF-2 the charges are generated in the bulk so that the majority of them are created well away from both surfaces. As a result, interface trapping is substantially reduced. Then, in a properly planned experiment (short electron pulse and not too strong electric fields to make transit times as long as possible) one can readily obtain the *intrinsic* current–time curve corresponding to a δ-pulse irradiation in a semi-infinite sample. Such data is indispensable for testing a theoretical model. Furthermore, using thinner samples and higher fields makes it possible to observe transit time effects to further test the theory.

In the framework of the Gaussian transport TOF to TOF-2 changeover is expected to result in a down sloping ramp [10]. Exactly this line of reasoning was used to prove the Gaussian transport of electrons in liquid hydrocarbons in the 1960 and 1970s [26] and the dispersive charge transport in MDP and PVK [1] (and in photoconductive chalcogenide glass As_2Se_3 [27]).

Dispersive transport leads to a power-law dependence $j \propto t^{-1+\alpha}$ for the pre-flight part of the transient to be replaced by a similar algebraic dependence $j \propto t^{-1-\alpha}$ for the post-flight times (see [10–12]). As indicated in section 3.1 (figures 2, 5 and 6) these predictions of theory are indeed verified for $\alpha = 0.75$.

In addition, the theory demands that TOF t_tr is longer than TOF-2 by a factor of $(\sqrt{3})^{1/\alpha}$ (2.08 for $\alpha = 0.75$) [10]. Again, there is a satisfactory agreement between theory and experiment (25 and 54 ms on figure 6). The same conclusion applies to appropriate times in figures 2 and 5 but the difference is somewhat greater. The problem here is that the standard expressions in MT theory (the so-called τ approximation [28]) hold only for $\alpha \leqslant 0.5$ whereas for larger α (our case) their accuracy is greatly compromised.

Now let us see what happens once electron energy starts to increase. The generation zone grows into the bulk of the MDP, causing the relative number of near-surface-generated carriers to diminish, leading in turn to the attenuation of surface effects once the maximum electron range leaves the surface layer. Of course, there is the concomitant shortening of the drift length. This in turn shortens the time of flight.

To check this idea we performed numerical calculations using the published theoretical results as a coordinate Green function to obtain the sought solution as in [10]. First, we treat the case of the true Gaussian transport featuring constant mobility and diffusivity (convection–diffusion problem). The rigorous solution has been found in [20] but for our purpose we may use a much simpler expression widely used in the literature (see [29], for example).

Figure 9 shows the effect of varying generation zone. As its length progressively increases, the plateau shortens but still

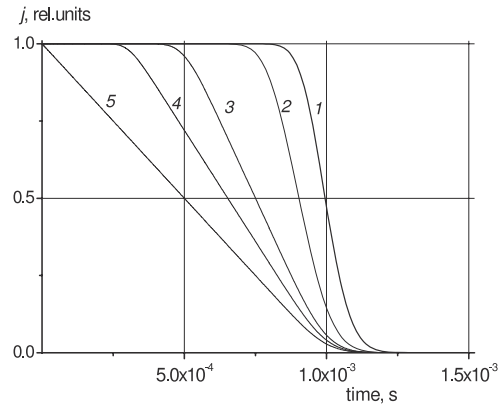

Figure 9. Computed TOF curves for the truly Gaussian transport. Thickness of the generation zone in units of the sample thickness (η): 0 (1), 0.2 (2), 0.5 (3), 0.7 (4) and 1.0 (5). Time of flight for curve (1) is 0.98 ms.

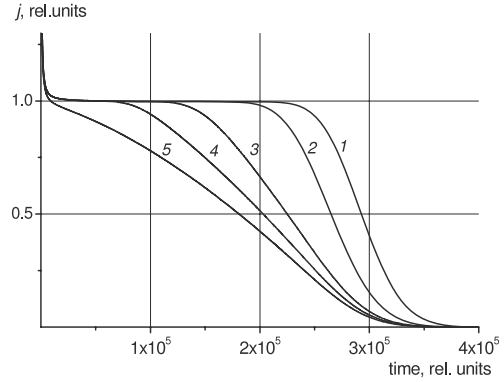

Figure 10. As figure 7 but for MT model with box-type trap distribution. Parameters of the model are such that the non-equilibrium phase of the carrier transport (initial spike) is short compared to the time of flight (here 2.97×10^5 in relative units).

stays. Of course, once the generation zone encompasses the whole sample (TOF-2 case) the plateau disappears and gives way to a down sloping ramp (a fact well known in the radiation chemistry of gases and liquids [26]).

To treat the more general model envisioning the dispersive to Gaussian transition we used the analytical solution obtained by Rudenko and Arkhipov for a box-type trap distribution [30] as in [12]. As figure 10 demonstrates, the only significant change compared to the previous analysis is an initial spike of short duration, which stays constant as long as the plateau still exists. The tail is gradually increasing in accordance with plateau shortening. These findings are of fundamental importance.

Let us now compare these theoretical predictions with data in figure 7. The transient shape (initially flat plateau) is seen to change drastically (curves 1–4) as the relative length of the generation zone increases to less than one-half of the sample thickness. It is remarkable that the time of flight for curve 1 ($t_0 = 9.74$ ms) is indeed larger than for curve 4 (8.2 ms) with W almost constant. For curve 5, on the other hand, l_m exceeds the sample thickness (TOF-2) and the transient acquires all the features of the dispersive transport.

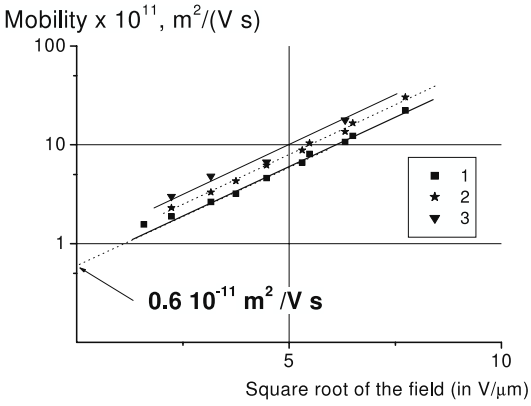

Figure 11. Field dependence of the drift mobility in sample no. 2. Method of measurement: TOF (1, 2) using standard double linear approach (1) and formally identifying the time of flight with the time of the crest of the cusp (2); TOF-1a (3) with electron energy 23 keV.

In figure 8 the transients start from a cusp and transform to a shoulder somewhere at 13 keV ($l_m \approx 4.1$ μm so that $l_m/L = 0.23$). Curve 6 already displays dispersive-type behavior though l_m/L is only 0.64. These results clearly show that hole transport in 30% DEH:PC is by no means Gaussian. In combination with TOF-2 results, we conclude that hole transport is dispersive.

The noticeable changes in a TOF transient form occur at an electron energy 8–12 keV (l_m is 2–4 μm), revealing that the generation zone starts to enter the bulk. This estimate of the surface layer thickness agrees with published results [31].

In this context, it is appropriate to remember experiments intended to test mobility thickness dependence [19, 32]. Here the TOF transient shape was not affected and the fact that time of flight scaled with the sample thickness ($t_{tr} \propto L$) was interpreted as a clear indication of the Gaussian transport. But those experiments did not touch upon the central feature of the TOF technique, namely the surface generation of charge carriers.

TOF-1a is a very efficient decider of the standing controversy about charge transport in MDP. Indeed, once the TOF curve manifests a flat plateau suggestive of the Gaussian transport one needs only to go to 20 keV energy in steps to check whether the plateau still stays (if only shortened). The positive outcome of this experiment surely proves the Gaussian nature of the transport. If not, the answer should be negative.

It should be remembered that in our earlier paper [33] we made a comparison between two varieties of the TOF method based on electron gun and laser, respectively, and have shown that basically there are no differences in transient shapes. Also, it should be remembered that dispersive transport has been shown to occur in 30% TTA:PS which, unlike 30% DEH:PC, features a non-polar polymer matrix and non-polar additive [34].

4.2. Field effects

Once it has been established that carrier transport in the studied MDP is mildly dispersive and the current transients observed

by TOF-2 and TOF-1a (and partly TOF) are in agreement with predictions of the MT or SM models it is necessary to test theoretical predictions concerning the field dependence of the carrier mobility. Earlier, we found that this dependence is close to MT predictions [11, 35, 36] and, at strong fields, runs contrary to the PF dependence as presented in [37, 38]. So, it came as a surprise that in the tested MDP mobility field dependence followed very closely the Poole–Frenkel law (figure 11). While these two laws are almost indistinguishable within experimental uncertainty at moderate fields (0.5×10^6–1×10^7 V m^{-1} [10]), they clearly start to diverge at fields exceeding 2×10^7 V m^{-1}.

This contradiction is of fundamental importance. Even if samples have been prepared in different laboratories the final tests have been conducted at the same facility. As a result, it was established that all samples featured close values of the drift mobility at 10^7 V m^{-1} and the dispersion parameter α (0.7 in our earlier works and 0.75 now). The discrepancy mainly concerns the value of the drift mobility at high fields only and rises with field. Now we have to understand what makes MDP samples prepared at the Vannikov Laboratory rather different in this respect (by the way, these samples had Al foils 100 μm thick as substrates and Al electrodes as well). The work in this direction is now in progress.

5. Conclusions

(1) Some innovations made it possible to settle the long-standing controversy regarding the charge carrier transport in DEH-doped PC which may be regarded as a typical MDP combining a polar polymer matrix with a polar dopant. First, introduction of an electron gun source allowed us to apply TOF-2 (bulk generation) and subsequently TOF-1a (variable generation zone) techniques to clarify this confusing situation. Second, we measured TOF transients over a wide dynamic range and analyzed them using log–log plots. Both these factors definitively proved the dispersive rather than Gaussian transport in this material, despite the fact that TOF transients featured a well-defined plateau (including flat ones) when viewed on a linear–linear scale.

(2) As similar results have been obtained for another typical MDP, namely 30% TTA:PS, which combines a non-polar matrix and a non-polar additive, it may be tentatively concluded that dispersive transport is a common feature of all MDP.

(3) In view of the two previous conclusions it seems rather strange that in tested samples of 30% DEH:PC there prevails a Poole–Frenkel field dependence of mobility. Our earlier results with samples of the same MDP prepared at the Vannikov Laboratory obeyed an algebraic dependence expected for a dispersive transport. Work to unravel this controversy is now in progress.

Acknowledgments

The authors would like to acknowledge discussions with L B Schein and samples provided by David Weiss from Eastman Kodak Company.

References

[1] Scher H and Montroll E W 1975 *Phys. Rev.* B **12** 2455
[2] Arkhipov V I, Iovu M S, Rudenko A I and Shutov S D 1979 *Phys. Status Solidi* a **52** 67
[3] Bässler H 1981 *Phys. Status Solidi* b **107** 9
[4] Bässler H 1993 *Phys. Status Solidi* b **175** 15
[5] Borsenberger P M and Weiss D S 1998 *Organic Photoreceptors for Xerography* (New York: Dekker)
[6] Mirchin N R and Peled A 2004 *HAIT J. Sci. Eng.* **1** 782
[7] Schein L B and Tyutnev A P 2008 *J. Phys. Chem.* C **112** 7295
[8] Pfister G 1977 *Phys. Rev.* B **16** 3676
[9] Pfister G and Scher H 1977 *Phys. Rev.* B **15** 2062
[10] Tyutnev A P, Saenko V S, Pozhidaev E D and Kolesnikov V A 2006 *J. Phys.: Condens. Matter* **18** 6365
[11] Tyutnev A P, Saenko V S, Kolesnikov V A and Pozhidaev E D 2005 *High Perform. Polym.* **17** 175
[12] Tyutnev A P, Saenko V S, Pozhidaev E D and Ikhsanov R Sh 2008 *J. Phys.: Condens. Matter* **20** 215219
[13] Gruenbaum W T, Lin L-B, Magin E H and Borsenberger P M 1997 *Phys. Status Solidi* b **204** 729
[14] Borsenberger P M, Cowdery-Corvan J R, Magin E H and Sinicropi J A 1997 *Thin Solid Films* **307** 215
[15] Spear W E 1955 *Proc. Phys. Soc.* B **68** 991
[16] Gross B, Sessler G M and West J E 1974 *J. Appl. Phys.* **45** 2841
[17] Martin E H and Hirsch J 1972 *J. Appl. Phys.* **43** 1001
[18] Mack J X, Schein L B and Peled A 1989 *Phys. Rev.* B **39** 7500
[19] Borsenberger P M 1990 *J. Appl. Phys.* **68** 6263
[20] Hirao A and Nishizawa H 1996 *Phys. Rev.* B **54** 4755
[21] Pautmeier L T, Richert R and Bässler H 1989 *Phil. Mag. Lett.* **59** 325
[22] Pautmeier L T, Richert R and Bässler H 1989 *Phil. Mag.* B **63** 587
[23] Schein L B, Scott J C, Pautmeier L T and Young R H 1993 *Mol. Cryst. Liq. Cryst.* **228** 175
[24] Gross B, Gerhard-Multhaupt R, Labonte K and Berraissoul A 1984 *Colloid Polym. Sci.* **262** 93
[25] Tyutnev A P, Saenko V S, Kundina Yu F, Doronin A N, Zinchenko V F and Pozhidaev E D 2005 *High Energy Chem.* **36** 300
[26] Hummel A and Schmidt W F 1974 *Radiat. Res. Rev.* **5** 199
[27] Monroe D and Kastner M A 1986 *Phys. Rev.* B **33** 8881
[28] Arkhipov V I 1993 *J. Non-Cryst. Solids* **163** 274
[29] Richert R, Pautmeier L T and Bässler H 1989 *Phys. Rev. Lett.* **63** 547
[30] Rudenko A I and Arkhipov V I 1978 *J. Non-Cryst. Solids* **30** 163
[31] Haridoss S and Perlmann M M 1983 *J. Appl. Phys.* **55** 1332
[32] Yuh H-J and Stolka M 1988 *Phil. Mag.* B **58** 539
[33] Kolesnikov V A, Tyutnev A P, Saenko V S and Pozhidaev E D 2006 *Polym. Sci.* A **48** 46
[34] Tyutnev A P, Saenko V S, Ikhsanov R Sh, Abramov V N and Pozhidaev E D 2008 *High Energy Chem.* **42** 29
[35] Tyutnev A P, Saenko V S and Pozhidaev E D 2004 *Khim. Fiz.* **23** 75 (in Russian)
[36] Tyutnev A P, Saenko V S and Pozhidaev E D 2006 *Polym. Sci.* B **48** 251
[37] Gill W D 1972 *J. Appl. Phys.* **43** 5033
[38] Schein L B, Rosenberg A and Rice S L 1989 *J. Appl. Phys.* **60** 4287